OSCILLATIONS OF THE INTERFACE TENSION INSIDE SOLIDS

A. Ya. Gokhshtein

UDC 541.1

So far the surface tension of solids [1-5] has been studied solely in the boundary between a solid electrode and an electrolyte. In paper [1] it was pointed out that this may be done in any interphase boundary. In the present study we investigated the tension of p-n-transitions in semiconductors. The experiments were done with 5 μ 15 mm single-crystal slabs in which a p-n-transition was created by diffusion from one or two sides, and on which films forming ohmic contacts were deposited on two sides. The main measurements were done in the following silicon samples. A) p-type, 2 $\Omega \cdot$ cm resistivity, transition from two sides (main and auxiliary) formed by diffusion of P, stratification depth of the main transition $\delta_1 = 7\ \mu$; contacts consisting of an Al coating, $\delta_2 = 5\ \mu$; total slab thickness $\lambda = 270\ \mu$ (Fig. 1). B) Transition from one side, $\lambda = 350\ \mu$, the other characteristics were identical to those of sample A (Fig. 2). C) n-type, 500 $\Omega \cdot$ cm resistivity, transition from one side formed by diffusion of B, $\delta_1 = 5\ \mu$, $\delta_2 = 5\ \mu$, $\lambda = 200\ \mu$. The shift in the transition $\varphi = \varphi_m + \Delta\varphi \sin \omega t$ (m index indicating the average, $\Delta\varphi$ amplitude) oscillates with the small amplitude $\Delta\varphi$ (criterion of smallness derived in [1]). The oscillations of the interface tension γ^0 thus generated produce vibrations in the system formed by the sample and a piezo-element, and the voltage generated in the faces of the piezo-element is recorded, the latter voltage being proportional to the variable component γ^0.

1. Although the samples examined possess quite special properties, we may still expect that, if no complications arise, the amplitude $\Delta\gamma^0$ of the first harmonic component of the voltage and the space charge ε of the transition will be related as follows $\Delta\gamma^0 = |\varepsilon|\Delta\varphi$, which relation is analogous to that for an electrode-electrolyte contact [1], the latter being derived by applying the Gibbs equation. Since ε rises when the constant negative displacement φ_m increases, this relationship predicts that the amplitude of the interface tension will rise with increasing φ_m. This conclusion is fairly well confirmed by the experiment. From the record shown in Fig. 1a, which was taken at decreasing voltage (from 0 to −8 V), at the frequency $\nu = 4800$ Hz and $\Delta\varphi = 0.8$ V, it follows that the interface tension (upper curve) increases markedly with φ_m. The curve representing the capacity of the current through the transition (second curve from the top) indicates that in this φ_m range the capacity of the transition $C(\varphi_m)$ is nearly constant, which agrees with the nearly linear rise of ε with φ_m (Fig. 1a). The experimental record of γ^0 versus φ_m is also nearly linear (Fig. 1a). Consequently, the ratio $\Delta\gamma^0/\Delta\varphi$ yields the sapce charge of the transition. The pseudocapacity produced by diffusion at low φ_m does not give rise to distortions.

2. According to the formula $\Delta\gamma^0 = |\varepsilon|\Delta\varphi$, the amplitude of the interphase tension does not depend on the frequency in the simplest case, whereas the current capacity rises with the frequency. The latter produces secondary effects in the bulk. Side effects can be eliminated by measuring at low frequencies where the current is small. Oscillograms of the interface tension $\Delta\gamma^0$, the current Δj, and the potential $\Delta\varphi$ at $\nu = 1190$ Hz are shown in Fig. 1b. The voltage was varied from +4.7 to −3.9 V. Since there exists a transition on the two sides of the slab, Fig. 1b should be considered to represent two plots which, exactly as those shown in Fig. 1a, were taken from $\varphi_m = 0$. The interval [−4.7 V, 0] corresponds to one transition and the interval [0, −3.9 V] to the other (left and right-hand sides of Fig. 1b). In each of the two records the opposite transition can be considered to represent a small additional resistance. This situation in the sample is favorable for measurements of $\Delta\gamma^0$ at $\varphi_m = 0$: 1) the direct current through the transition and the proportional side effects are small; 2) the periodical component of φ may be considered sinusoidal, although during one half-period it is applied mainly to one transition and during the other half-period to the opposite transition: the deformations of one and the same sign (elongation) which are produced on the opposite sides of the slabs during the two half-periods are equivalent to a sinusoidal deformation on one side (two-stroke system). The second condition is only partly fulfilled in the slab in which the records of Fig. 1 were taken, for, the transitions at the two sides are not of identical quality. The reverse current from the auxiliary transition and the variable component of this current (left-hand side of Fig. 1b) are of considerable magnitude. The

Institute of Electrochemistry, Academy of Sciences of the USSR (Presented by Academician A. N. Frumkin, Dedember 31, 1966). Translated from Doklady Akademii Nauk SSSR, Vol. 174, No. 3, pp. 394-397, May, 1967. Original article submitted November 23, 1966.

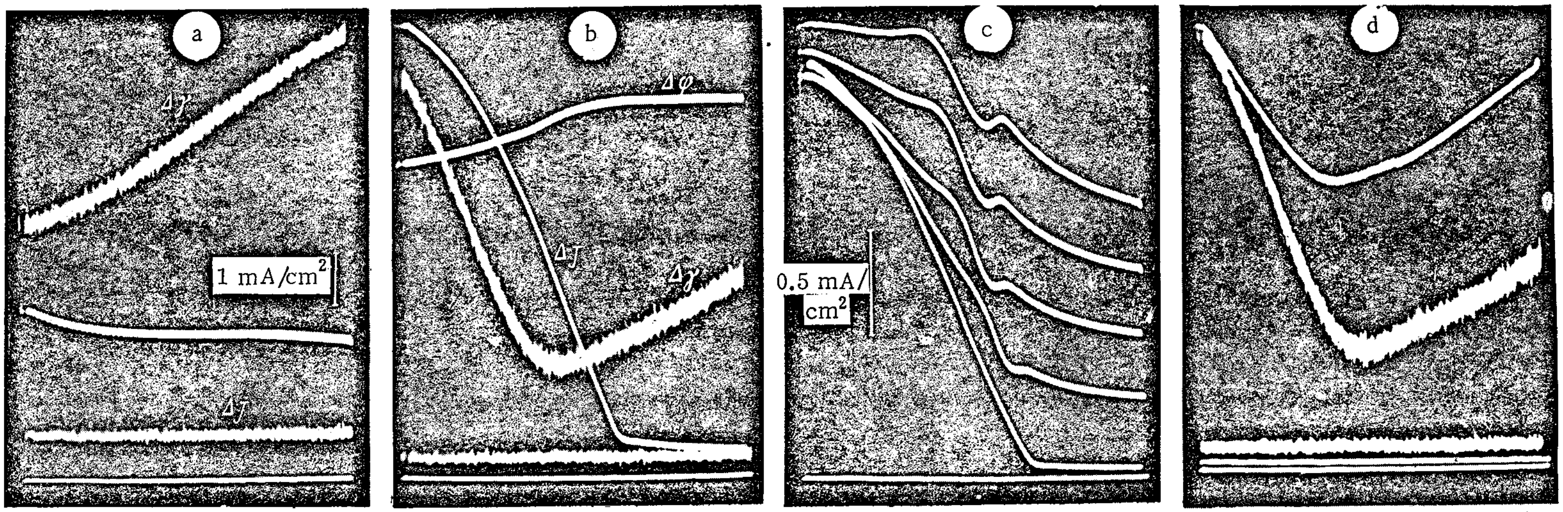

Fig. 1. Oscillations of the interphase tension in a p-n-transition at $\varphi_m < 0$; Si slab with two transitions; $|d\varphi_m/dt| = 0.12$ V/sec; R = 100 Ω. a) $\Delta\gamma$ and Δf at $0 < -\varphi_m < 8$ V, $\Delta v = 0.7$ V, $\nu = 4800$ Hz; b, c, d) axis of abscissas is divided into two regions: auxiliary transition (left-hand side, φ_m is varied from −4.7 to 0 V), main transition (right-hand side, φ_m is varied from 0 to −3.9 V), $\Delta v = 0.8$ V; b) $\Delta\gamma$, Δj, and $\Delta\varphi$, $\nu = 1190$ Hz; c) Δj at $\nu = 0.5, 5, 10, 15, 20$ kHz; d) $\Delta\gamma$ at $\nu = 1190$ Hz (bottom) and $\nu = 10020$ Hz. Lower horizontal line: reference level, line above this line: noise level of $\Delta\gamma$ (1.1 μV at 1190 Hz; 1.0 μV at 4800 Hz; 0.8 μV at 10020 Hz). In Fig. 1b, 1 μV ~ 0.054 dyn/cm (calibration).

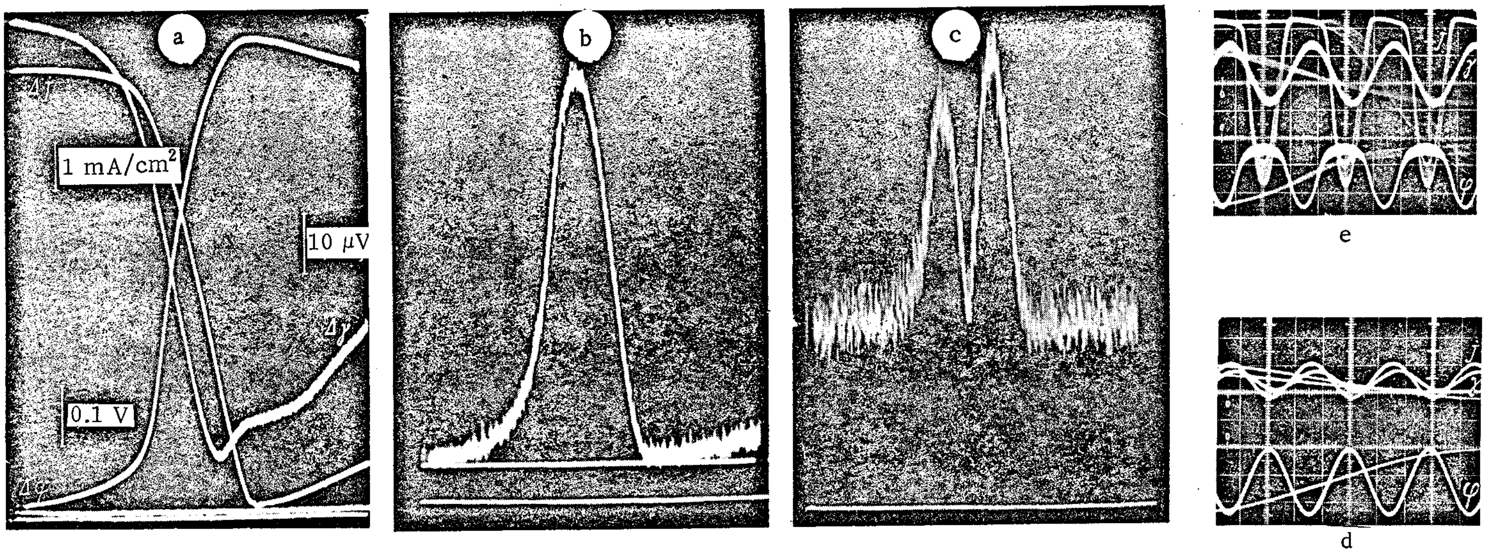

Fig. 2. Oscillations of the interphase tension in a p-n-transition and superposed thermoelectric vibrations at $\varphi_m > 0$; Si slab containing a single transition and immersed in alcohol; R = 110 Ω, $\Delta\nu$ = 0.8 V. a, b, c) $|dv_m/dt|$ = 0.12 V/sec, v_m is varied from +4.7 (left-hand side) to −3.9 V; a) $\Delta\gamma$ (first harmonic), Δj, $\Delta\varphi$, ν = 1760 Hz; b) $\Delta\gamma_2$ (second harmonic): $\Delta\gamma$ at the frequency ν = 1760 Hz and $\nu_\varphi = \nu/2$ = 880 Hz; c) $\Delta\gamma_3$ (third harmonic), ν = 1760 Hz, $\nu_\varphi = \nu/3$ = 587 Hz, horizontal region of $\Delta\gamma_3$ corresponds to the noise level (1 mV); d) $\gamma(t)$, $j(t)$, $\varphi(t)$, ν = 4000 Hz, φ_m = 0.8 V; e) same function, φ_m = 4.7 V, force j, γ tenfold reduced, and φ tenfold amplified, phase shift: at φ_m = 3.9 V the phases of γ and φ are identical. In Fig. 2a, 1 mV ~ 0.030 dyn/cm (scale of Fig. 1b).

reverse current from the main transition (right-hand side of Fig. 1b) is very small. Fig. 1c shows the current passing through the slab at the same φ_m and frequencies equal to 0.5, 5, 10, 15, and 20 kHz. The alternating current passing through the main transition (right-hand side of Fig. 1c) is proportional to the frequency; the phase shift referred to the potential equals $\pi/2$, i.e., this current is almost entirely due to a capacity. Therefore, the conditions at which $\Delta\gamma^0$ is proportional to ε are fulfilled for the main transition (entire Fig. 1a, right-hand parts of Fig. 1b, c, d). At 1190 Hz the current from the main transition is already sufficiently small, and the distortions produced by side effects (methods of estimating these effects are discussed below) do not exceed 10% of the measured $\Delta\gamma$ value. Calibration by means of the method of paper [5] yields $\Delta\gamma^0 = 0.64$ dyn/cm at $\varphi_m = -3.9$ V; differentiation of $\Delta\gamma^0/\Delta\varphi$ with respect to φ_m (Fig. 1b)* yields $C = 1.1 \cdot 10^{-2}$ μF/cm^2, whereas from the plot of the current (Fig. 1c) at $\varphi_m = -3.9$ V it follows that $C = 1.3 \cdot 10^{-2}$ μF/cm^2. The side effects, which are proportional to the capacity increase with rising frequency, which causes the $\Delta\gamma$ versus φ_m curve to shift. In Fig. 1d oscillograms of $\Delta\gamma$ and φ_m at 1190 and 10020 Hz are plotted along different scales.

3. The range of positive shifts was studied in slabs with a single transition (Fig. 2). To keep the temperature constant at large direct currents, the slab was immersed in alcohol during the measurements. Passing from positive to negative φ_m values (from left to right in Fig. 1a), we note the following regions of the curve of $\Delta\gamma$ versus φ_m. I) $\Delta\gamma$ is low and drops slightly; an increase of the frequency is accompanied by a noticeable decrease of $\Delta\gamma$ in this region. II) A steep drop of $\Delta\gamma$. III) A minimum with symmetrical branches around the minimum $\Delta\gamma$. IV) Linear rise of $\Delta\gamma$. V) Accelerated rise. Records of Δj and $\Delta\gamma$ are shown in Fig. 2a. The regions of high $\Delta\gamma$ and high Δj coincide. In the latter region $\Delta\gamma$ is only approximately proportional to Δj. Inclusion of a resistance R in series with the transition at a constant amplitude Δv of the voltage applied to the two ends of the chain enables us to create a region of constant Δj (right-hand side of Fig. 2a) in the range $\varphi_m >> 0$; the magnitude of this constant current depends on R. In contrast to Δj, $\Delta\gamma$ varies noticeably in this region. The drop of $\Delta\gamma$ in the beginning of region II is steeper than that of Δj.

4. The following effects may result in a further bending of the slab superposed on the bending produced by the change in interfacial tension. 1) A piezoelectric effect generated in the bulk of the semiconductor by a field proportional to the current. An estimate shows that this effect is small in our case; a piezoelectric effect is generated in the layer where the space charge is located at $\varphi_m < 0$; it is independent of φ_m, Δj and ν and is responsible for a small shift of the zero reference line. 2) Considerable heating of the layer with the higher resistivity. In our case this effect is negligible at $\varphi_m > 0$; at $\varphi_m < 0$ the same holds mainly for the heating of the transition by the reverse current; according to estimates, this effect is of second order, and manifests itself only at a high reverse current and moderate frequencies. 3) Injection of minority current carries, which lowers the resistivity of the slab layer adjacent to the transition; calculation and experimental study of the relationship between $\Delta\gamma$ and j_m show that this effect is small. 4) Thermoelectric heating and cooling of the opposite sides of the slab are the main causes of the oscillations of the internal stresses superposed on the oscillations of the voltage; at $\varphi_m > 0$ this is the Peltier effect; at $\varphi_m < 0$ this explains why the thermoelectric effects produced by the passage of current carriers into and from the space charge region are different; this effect is considerable under nonstationary conditions. The change in the shift towards the positive side of the transition has the following consequences: a) the charge is reduced ($\varepsilon < 0$ at any φ_m) and the interface tension reinforced, so that the transition is linearly compressed, b) the contact is heated, with the result that the layers adjacent to the transition expand. Hence, it follows that the deformations produced under stationary conditions by the changes in the interface boundary and the temperature of the transition are of opposite sign. At low frequencies the phase difference comes close to π. Let the voltage be $v = \varphi + jSR = v_m + \Delta\, v\sin\omega t$, the density of the current through the slab $j = j_m + \Delta\, j\sin(\omega t + \theta)$ (S denotes the area of one side of the slab, t the time, $\omega = 2\pi\nu$), and the variable components of the heat flow: $\tilde{q}_1 = \pi_1(j - j_m)$ on one side, $\tilde{q}_2 = -\pi_2(j - j_m)$ on the other side (in the special case, π_1 and π_2 are the Peltier coefficients); analysis shows that the slab will oscillate as if there were the following variable interface tension on one side of the slab:

$$\gamma(t) = (\varkappa E/\zeta\rho)(\lambda^2/12a^2)(\Pi_1 + \Pi_2)\Delta j Q(\beta)\sin[\omega t - \psi(\beta) + \theta + \pi],$$
$$Q(g = \tan\beta,\ h = \operatorname{th}\beta) = 3\{{}^1/_2 h^2(1+g^2)^2 + {}^1/_2 g^2(1-h^2)^2 + \beta^2(1+g^2h^2)^2 - \beta[h(1+g^2) + g(1-h^2)](1+g^2h^2)\}^{1/2}/2\beta^3(1+g^2h^2), \quad (1)$$
$$\psi(\beta) = \arctan\frac{2\beta(1+g^2h^2) - h(1+g^2) - g(1-h^2)}{h(1+g^2) - g(1-h^2)},$$

* Calculation for a thin p-n-transition yields the formula $d\gamma/d\varphi = -\varepsilon/2(1-\mu)$, where μ denotes the Poisson coefficient (0.2-0.3).

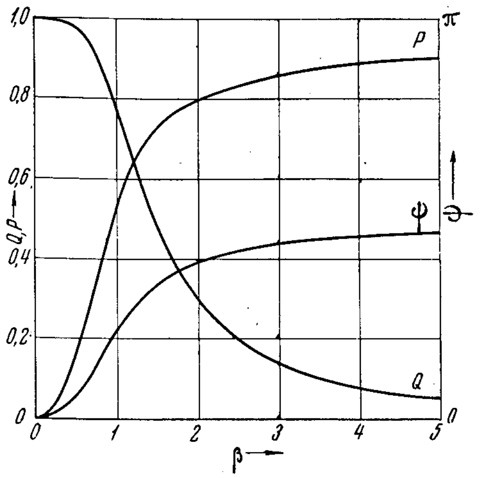

Fig. 3. Functions Q(β), ψ(β), and P(β) = $\Delta\bar{\gamma}/\Delta\gamma^-_\infty$; $\beta = (\lambda/2a)\sqrt{\omega/2}$.

the argument $\beta = (\lambda/2a)\sqrt{\omega/2}$; $Q(0) = 1$, $\psi(0) = 0$, $Q(\infty) = 0$, $\psi(\infty) = \pi/2$ (Fig. 3); $\varkappa$ denotes the coefficient of linear expansion, ζ the heat capacity, ρ the density, a^2 the coefficient of thermal conductivity, E the elasticity modulus (in Si: $\varkappa = 4.2 \cdot 10^{-6}$ deg^{-1}, $\zeta = 0.71$ J/g · deg, $\rho = 2.33$ g/cm³, $a^2 = 0.88$ cm²/sec [6], the Peltier coefficients π are of the order of tens of volts, $E = 0.84 \cdot 10^{12}$ dyn/cm² (static bending tests)). At Δj = const (at $\varphi_m > 0$, mainly $j^+ = v/R$, $\theta = 0$) $\Delta\gamma^+$ drops below the $\Delta\gamma_0^+$ value given by [1] when ω rises. The phase γ^+ with reference to the phase of the tension γ^0 (and v) varies from π at $\omega = 0$ to $\pi/2$ at $\omega \to \infty$. At $\Delta j = -\omega C\Delta\varphi$ (at $\varphi_m < 0$, essentially $j^- = C\, dv/dt$, $\theta = \pi/2$) γ^- increases from zero at $\omega = 0$ to $\Delta\gamma^-_\infty = 2(\varkappa E / \zeta\rho)C\Delta\varphi\Pi$. At the same time the phase of γ^- varies from $3\pi/2$ to π.

5. The considerations exposed above explain the shape of the $\Delta\gamma$ versus $\varphi_m(v_m)$ curve (Fig. 2a) and the variation with the frequency. Since the difference between the phases of γ^+ and γ^0 at low frequencies is close to π, the gradual rise of $\Delta\gamma^+$ with φ_m at first reduces the total $\Delta\gamma$ signal; the latter signal passes through a minimum ($\Delta\gamma_{min}$) and starts rising after the condition $\Delta\gamma^+ > \Delta\gamma^0$ is fulfilled; $\Delta\gamma_{min} \neq 0$, since the difference between the phases of γ^+ and γ^0 is less than π. The phase difference decreases with rising ω, which causes $\Delta\gamma_{min}$ to increase. The steep drop of $\Delta\gamma^+$ with rising ω shifts the minimum towards positive φ_m · $\Delta\gamma^0$ decreases with rising positive φ_m; hence, the phase difference $\Delta\gamma \approx \Delta\gamma^+ - \Delta\gamma^0$ rises faster (region II) than Δj. The steep rise of $\Delta\gamma$ at large negative φ_m is not related to the Peltier effect produced by the rising reverse current; the absence of a characteristic minimum indicates that the phase of the observed effect is nearly equal to the phase of the voltage; this effect is produced by the heating of the transition by the reverse current j_r and can be estimated from the power $|\Delta j_r \varphi_m|$. Comparison of the maximum γ and $j(\varphi_m = 4.7$ V) for sinusoidal variations (Fig. 2b, c, e) shows that the values at negative φ_m and minimum current (Fig. 2a) are about ten times higher than those which might be produced by the current. The same holds for $\Delta\gamma$ and its variation with rising φ_m as shown in Fig. 1a, b. For example, the effect of the reverse current ($\varphi_m = -3.9$ V, $\Delta j_r < 10$ μA/cm²) is about one hundredth of the difference $\Delta\gamma(-3.9) - \Delta\gamma(0)$. The main features of the phenomena described above for Si were found also in preliminary experiments with Ge.

LITERATURE CITED

1. A. Ya. Gokhshtein, Zav. Lab., 32, 815 (1966).
2. A. Ya. Gokhshtein, Avt. Svid. No. 178161, Byull. Izobr., No. 2 (1966).
3. A. Ya. Gokhshtein, Avt. Svid. No. 179043, Byull. Izobr., No. 4 (1966).
4. A. Ya. Gokhshtein, Élektrokhimiya, 2, 1061 (1966).
5. A. Ya. Gokhshtein, Élektrokhimiya, 2, 1318 (1966).
6. J. A. Carruthers, T. H. Geballe et al., Collection: Silicon [Russian translation (1960), p. 248.